

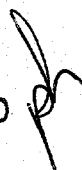
KAPL-P-000114
(K98155)

INFLUENCE OF DISSOLVED HYDROGEN ON NICKEL ALLOY
SCC IN HIGH TEMPERATURE WATER

CONF-990301--

D. S. Morton, S. A. Attanasio, J. S. Fish, M. K. Schurman

March 1999

DISTRIBUTION OF THIS DOCUMENT IS UNLIMITED 

MASTER

NOTICE

This report was prepared as an account of work sponsored by the United States Government. Neither the United States, nor the United States Department of Energy, nor any of their employees, nor any of their contractors, subcontractors, or their employees, makes any warranty, express or implied, or assumes any legal liability or responsibility for the accuracy, completeness or usefulness of any information, apparatus, product or process disclosed, or represents that its use would not infringe privately owned rights.

KAPL ATOMIC POWER LABORATORY

SCHENECTADY, NEW YORK 12301

Operated for the U. S. Department of Energy
by KAPL, Inc. a Lockheed Martin company

DISCLAIMER

This report was prepared as an account of work sponsored by an agency of the United States Government. Neither the United States Government nor any agency thereof, nor any of their employees, makes any warranty, express or implied, or assumes any legal liability or responsibility for the accuracy, completeness, or usefulness of any information, apparatus, product, or process disclosed, or represents that its use would not infringe privately owned rights. Reference herein to any specific commercial product, process, or service by trade name, trademark, manufacturer, or otherwise does not necessarily constitute or imply its endorsement, recommendation, or favoring by the United States Government or any agency thereof. The views and opinions of authors expressed herein do not necessarily state or reflect those of the United States Government or any agency thereof.

DISCLAIMER

Portions of this document may be illegible in electronic image products. Images are produced from the best available original document.

INFLUENCE OF DISSOLVED HYDROGEN ON NICKEL ALLOY SCC IN HIGH TEMPERATURE WATER

D.S. Morton, S.A. Attanasio, J.S. Fish and M.K. Schurman

Lockheed Martin
P.O. Box 1072
Schenectady, NY 12301

ABSTRACT

Stress corrosion crack growth rate (SCCGR) tests of nickel alloys were conducted at 338°C and 360°C as a function of the hydrogen concentration in high purity water. Test results identified up to a 7x effect of hydrogen levels in the water on crack growth rate, where the lowest growth rates were associated with the highest hydrogen levels. At 338°C, the crack growth rate decreased as the hydrogen levels were increased. However, different results were observed for the test conducted at 360°C. As the hydrogen level was increased in the 360°C tests, the crack growth rate initially increased, a maximum was exhibited at a hydrogen level of ~ 20 scc/kg, and thereafter the crack growth rate decreased. Based on this testing and a review of the commercial literature, the thermodynamic stability of nickel oxide, not the dissolved hydrogen concentration, was identified as a fundamental parameter influencing the susceptibility of nickel alloys to SCC. These test results are discussed in relation to the accuracy of extrapolating high temperature SCC results to lower temperatures.

INTRODUCTION

Hydrogen is often added to high temperature water to maintain low levels of dissolved oxygen and thereby minimize corrosion of structural materials. Several researchers have shown that hydrogen dissolved in high temperature water (360 °C) or hydrogen gas in steam (400 °C) affects the stress corrosion cracking (SCC) performance of alloy 600. Excellent reviews on the influence of hydrogen additions on SCC of nickel-base alloys have been provided by Cassagne et al.¹ and Pathania and McIlree.²

Magnin et al.³ and Economy and Pement.⁴ showed that the initiation time for SCC in reverse U-bend (RUB) samples of alloy 600 initially decreased as the dissolved hydrogen content increased. However, further increases in the hydrogen content of the water above a critical level decreased

the severity of SCC. A similar effect of hydrogen overpressure on the extent of intergranular cracking was observed during constant extension rate tests on alloy 600 in 360 °C water. Cassagne and Gelpi⁵ showed that the crack growth rate of alloy 600 in high temperature water (360 °C) also exhibits a maxima at a critical concentration of hydrogen.

Based on these studies, it appears that hydrogen dissolved in water (over the temperature range of 360 °C to 400 °C) is initially detrimental to the SCC resistance (both initiation and growth) of alloy 600, but above a certain level may actually improve SCC performance. However, few systematic studies have investigated the influence of hydrogen on SCC growth at temperatures below 360°C. This paper presents the results of tests measuring the effect of dissolved hydrogen concentration on the SCC growth rate of alloys 600 and X-750 at temperatures of 338°C and 360°C.

EXPERIMENTAL PROCEDURE

The nickel alloys investigated in this study were mill annealed alloy 600, alloy X-750 condition HTH, and alloy X-750 condition AH. The compositions for these alloys are provided in Table 1. The alloy 600 was fabricated into standard 25.4 mm compact tension (CT) specimens with 10% side grooves and the X-750 was fabricated into standard 10.2 mm CT specimens. All specimens were fabricated in an longitudinal-transverse (LT) orientation. Test specimens were air fatigue precracked, to a nominal a/W of 0.5 for alloys 600 and X-750 AH and 0.45 for alloy X-750 HTH, using the fatigue precracking procedure from ASTM E399 Annex 2. The alloy X-750 tests were conducted under pure constant load test conditions, whereas a 10% daily unload was performed in the alloy 600 test. The initial nominal stress intensity factor (K_I) in the alloys 600 and X-750 AH tests was 27.5 MPa \sqrt{m} , and 49.4 MPa \sqrt{m} in the alloy X-750 HTH tests.

Constant load stress corrosion crack growth rate (SCCGR) tests were conducted with Instron 8562 servoelectric machines with Model 8500 digital control electronics monitored through a LabVIEW computerized data acquisition system. A description of the recirculating high flow rate autoclave system has previously been described.⁶ Crack lengths were monitored in-situ using electrical potential drop (EPD) according to ASTM E647, Annex 3, and were verified by post-test destructive examinations (DE). Alloy 600 EPD measured active voltages (proportional to crack extension) were normalized for alloy 600 resistivity changes measured in an unloaded non-precracked 10.2 mm CT specimen of the same heat. Since alloy X-750 resistivity does not change appreciably with time⁷, X-750 EPD resistivity normalizations were not performed in tests with these materials.

Test Environment

The SCCGR test chemistries were deaerated high purity water with various levels of dissolved hydrogen. The feed tank solution was buffered to a room temperature pH of 10.1 to maintain a near neutral autoclave pH at the test temperature. Separate tests were performed at multiple hydrogen concentrations for alloys X-750 AH and HTH (between 1 and 149 scc/kg) and at 120 scc/kg for alloy 600. The desired hydrogen concentrations were obtained by varying the feed tank

hydrogen overpressure according to Henry's law. A Henry's law coefficient of 5.9 kPa/(scc/kg), the solubility of hydrogen in water at 25°C, was used for these room temperature calculations. Cylinders of mixed gas containing 4% or 14.7% hydrogen, with the balance argon, were used to obtain hydrogen levels less than 20 scc/kg. Since the autoclave turnover rate is relatively rapid (once every hour), autoclave effluent dissolved gas levels are analogous to feed tank levels, and the oxygen levels for all tests were <10 ppb.

Alloys 600 and X-750 AH tests were conducted at 338°C and alloy X-750 HTH tests were conducted at 360°C. Prior to the start of the alloys 600 and X-750 AH SCC tests, test specimens were prefilmed in the load train for 10 and 14 days, respectively, at $K_I \cong 4 \text{ MPa}\sqrt{\text{m}}$ and 260°C at the hydrogen level of the SCC test. Alloy X-750 HTH specimens were not prefilmed. The differences in material prefilming procedures were a consequence of historical testing practices.

Trends in facility pH buffer and contaminant levels were monitored through system in-line conductivity probes. Absolute anion contaminant levels were verified as less than detectable (~ 25 ppb) by ion chromatography (IC) analysis of autoclave effluent samples. Autoclave cation contaminants were monitored through analysis of autoclave effluent samples by inductively coupled plasma spectroscopy (ICP). Cation contaminant levels typically coincided with at temperature cation solubility limits (e.g., ~ 2 ppb Fe).

Upon completion of SCC testing, alloys 600 and X-750 AH test specimens were heat-tinted at 454°C in air for 8 hours for fractography. Following heat-tinting, the alloy 600 specimen underwent an air fatigue extension. This process avoids deformation of the SCC surface during post test fracture of the specimen. The higher strength 10.2 mm alloy X-750 CT specimens, as well as the fatigue extended alloy 600 specimen, were ultimately pulled apart in tension to expose the fracture surfaces. The amount of SCC in each specimen was measured by optical examination using the procedure in ASTM E813.

RESULTS

SCCGR Analysis

Electrical potential drop (EPD) indicated immediate SCC growth at the start of all tests. Consequently reported crack growths were determined by dividing the actual destructive examination (DE) intergranular SCC extension by the test duration. Actual crack extensions were consistently underpredicted by EPD by a factor ranging from 1.5 to 3. This under prediction occurs consistently for materials with branched crack fronts and results from uncracked metal ligament conduction paths. EPD would have dramatically over predicted the actual alloy 600 crack extension if material resistivity increase was not accounted for.

Influence of Hydrogen on SCCGR

Results from this testing discerned a dramatic effect (up to 7x) of dissolved hydrogen on SCCGR. Figures 1 and 2 show the influence of hydrogen on the SCCGR of alloys X-750 AH and HTH, respectively. Each point in these figures represents a single specimen tested at a unique constant hydrogen level except for the 35 and 67 scc/kg symbols in Figure 1 and the 50 scc/kg symbol in Figure 2. The 35 and 67 scc/kg symbols in Figure 1 represent the means of 3 and 10 specimens, respectively. The 50 scc/kg symbol in Figure 2 is the mean of 22 specimens from 9 separate tests.

Confidence intervals of 95% for the reported means and the single SCCGRs were estimated from the variances of the multiple specimen tests. At 338°C, X-750 AH exhibits a monotonically decreasing SCCGR with increasing hydrogen level until about 40 to 50 scc/kg. Hydrogen concentration above this transition level have no further effect on SCCGR. At 360°C, X-750 HTH also exhibits a decreasing SCCGR with increasing hydrogen levels above ~20 scc/kg. The saturation hydrogen level for which further hydrogen level increases have no SCCGR effect is ~80 scc/kg at this temperature. However, a dramatic difference in SCCGR behavior was observed at the two temperatures for hydrogen levels less than ~20 scc/kg. SCCGR increased with increasing dissolved hydrogen at 360°C for hydrogen levels less than 20 scc/kg, and SCCGR decreased with hydrogen additions at 338°C.

Influence of Hydrogen Concentration on Corrosion Potential

Figure 3 provides a comparison of measured (specimen and platinum) and predicted electrochemical corrosion potentials (ECPs) as a function of hydrogen level for each of the three temperatures tested (260°C preconditioning of alloy X-750 AH, 338°C for alloy X-750 AH and 360°C for alloy X-750 HTH). All corrosion potential measurements were measured with EPD off. Corrosion potentials were measured using an Fe/Fe₃O₄ reference electrode. This type of reference probe is sensitive to pH changes; thus measurements were converted to the standard hydrogen scale by subtracting 880 mV at 260 °C, 993 mV at 338 °C, and 1068 mV at 360 °C.⁽¹⁾ This figure illustrates, consistent with expectations,⁸ that nickel alloys and platinum behaved essentially as a hydrogen electrode for all hydrogen levels and temperatures tested. At lower hydrogen levels, platinum behaves more like a hydrogen electrode than the nickel alloys (i.e., platinum is a better catalyst than nickel and since it is inert, metal oxidation does not influence its ECP).

DISCUSSION OF RESULTS

Influence of Oxide Stability on SCC

As illustrated in Figures 1 and 2, hydrogen concentration is not the fundamental parameter which describes SCCGR (for increasing hydrogen levels below 20 scc/kg, SCCGR decreases at 338 °C and increases at 360 °C). Combrade⁹ and Rebak and Smialowska¹⁰ have suggested that the influence of hydrogen on SCC is fundamentally related to its influence on oxide stability. Nickel alloy primary water SCC crack tip oxides are predominately nickel oxide (NiO) with a cubic crystal structure.¹¹ As illustrated in Figure 4, nickel oxide undergoes a phase transition to nickel metal at hydrogen levels and temperatures of interest to this study. The transition hydrogen levels for 338 °C and 360 °C are ~45 and 80 scc/kg, respectively, are also presented in Figures 1 and 2.

The stability of an oxide may be described by the amount that the corrosion potential deviates

⁽¹⁾ 880, 993, and 1068 mVs are the standard potentials of the Fe/Fe₃O₄ half cell reaction using thermodynamic properties from References^{12,13} at the temperatures of 260 °C, 338 °C, and 360 °C (at temperature pHs of 6.6, 6.5, and 6.8, respectively).

from the potential corresponding to the thermodynamic stability of that oxide. Using this approach, the observed hydrogen SCCGR functionality, irrespective of temperature, should be characterized by the extent that the corrosion potential deviates from the potential of the Ni/NiO equilibrium (i.e., $ECP - ECP_{Ni/NiO}$). Figure 5 shows the measured crack growth rates (for three alloys and two temperatures) as a function of this new parameter which reflects the relative stability of nickel oxide. Figure 5 observed SCCGRs for each material have additionally been normalized by the slowest SCCGR for that material (1.8×10^{-10} m/s for alloy X-750 AH at 338°C and 106 scc/kg; 2.1×10^{-11} m/s for alloy 600 at 338°C and 120 scc/kg; 8.8×10^{-11} m/s for alloy X-750 HTH at 360°C and 107 scc/kg) such that all materials could be compared in the same figure. As illustrated by the characterization of all hydrogen SCCGR data in Figure 5, $ECP - ECP_{Ni/NiO}$ is an appropriate variable to describe hydrogen SCCGR effects for nickel alloys in high purity water.

Figure 5 indicates that the largest hydrogen SCCGR effect (5 to 7x increase) occurs at a corrosion potential approximately 30 to 80 mVs more anodic than the transition corrosion potential. Other researchers,^{1,9} have noted that SCC is often associated with changes in oxide stability and that the greatest susceptibility to cracking occurs at corrosion potentials adjacent to a region where oxide passivity changes, such as the thermodynamic stability of an oxide. Figure 5 denotes that as hydrogen levels are increased above this maximum (decreasing ECP) SCCGR is reduced until nickel metal is thermodynamically stable. SCCGR similarly decreases when hydrogen levels are decreased relative to the hydrogen level corresponding to this maximum. It is important to realize that at 338°C corrosion potentials greater than ~70 mV above the Ni/NiO corrosion potential are not physically possible in a hydrogenated water environment (i.e., the largest experimental anodic potential difference was 60 mV corresponding to 0.7 scc/kg hydrogen, see Figure 5).

Methodology to Determine SCC Thermal Activation Energy (Q)

The determination of an accurate SCC thermal activation energy (Q) requires that all fundamental parameters other than temperature must be maintained constant. SCCGR tests have traditionally been conducted at an approximately constant hydrogen concentration, regardless of temperature. However, the SCC results reported in this study show that a constant hydrogen level exerts a variable influence on crack growth rate depending on the temperature. This is caused by a change in the thermodynamic stability of the crack tip oxide (metallic nickel versus NiO), which is the fundamental basis for hydrogen's influence on SCC. Therefore, to obtain an accurate thermal activation energy, or to accurately extrapolate high temperature test results to lower temperatures, SCC tests should be conducted such that a single crack tip oxide is stable at all temperatures. For example, if the end use of Q is to predict SCCGRs for temperature/hydrogen regimes in which nickel metal is thermodynamically stable, then the elevated temperature accelerated tests should be conducted with hydrogen levels such that nickel metal is stable. Recall that SCCGR appears to be independent of dissolved hydrogen level within the nickel metal regime.

The possible implication of not keeping the crack tip oxide regime constant when extrapolating high temperature SCCGR results to lower temperatures where nickel metal is stable is illustrated in Figure 6. Based upon growth rates measured in this study, two Qs (one based upon constant hydrogen level testing and the other based on constant crack tip oxide regime testing) are determined in this figure. This figure, admittedly based on very limited data, illustrates that the Q determined from nickel metal regime testing could be as much as factor of 2 to 3 times smaller than the Q determined from constant hydrogen level testing. This difference in Q, Figure 6, gives rise to an approximate 2x difference in extrapolated SCCGR at 315°C and highlights the need for crack tip

oxide regime testing similitude.

Mechanistic Insight from Dissolved Hydrogen SCCGR Functionality

A cursory consideration of the observed hydrogen crack growth effect could lead to the conclusion that nickel alloy crack growth is not consistent with a hydrogen SCC mechanism. It could be argued that detrimental hydrogen within metals is solely due to hydrogen in the water and since crack growth rates eventually decrease with increasing dissolved hydrogen level a hydrogen mechanism is not viable. The flaw in this interpretation is that corrosion reactions (in addition to hydrogen in the water) can also contribute to the level of hydrogen within metals. However, for a hydrogen SCC mechanism to be consistent with the observed SCCGR hydrogen functionality, the dominant source of hydrogen within the metal must be through corrosion reactions (decreases in SCCGR were noted with increasing hydrogen level in the water). This hydrogen SCC mechanism constraint also implies that increased corrosion and subsequent metallic hydrogen pickup must have the same dissolved hydrogen concentration functionality as the observed crack growth.

It is interesting to note, to be consistent with the observed hydrogen SCCGR functionality, that corrosion must be a dominant SCC subprocess for hydrogen SCC mechanisms. With this restriction the engineering differences between SCC dissolution and hydrogen mechanisms are virtually indistinguishable, since the critical subprocess for both mechanisms is corrosion (source of hydrogen for hydrogen mechanisms and crack generator for dissolution mechanisms).

CONCLUSIONS

- Testing has identified a dramatic (up to 7x) effect of dissolved hydrogen level on the crack growth rate of nickel alloys. This growth rate effect has fundamentally been quantified by the extent that the alloy's corrosion potential deviates from the corrosion potential of the Ni/NiO phase transition. Crack tip oxides are a nickel oxide and this corrosion potential difference represents the relative stability of the crack tip oxide.
- An improved methodology to determine SCC thermal activation energies has been developed based upon the understanding gained in this study (i.e., elevated temperature testing should be performed within a constant crack tip oxide regime not at a constant dissolved hydrogen level).
- The observed influence of hydrogen on SCC suggests that if a nickel alloy hydrogen SCC mechanism is applicable then corrosion reactions not hydrogen dissolved in the water are the dominant source of detrimental hydrogen within metals.
- The hydrogen SCCGR effect is a factor which has contributed to the scatter in SCC growth rate data. Careful control of SCC test hydrogen levels could eliminate some of the data scatter observed. It is the authors' expectation that other SCC growth rate scatter reductions, as well as key SCCGR functional identifications, may be obtained through well controlled testing.

ACKNOWLEDGMENT

The authors would like to thank the following individuals for their contribution to this effort: Nathan Lewis and Walter Yang for their AEM analysis. Mark Ando, John Anderson, Sergio Gonzalez and Wayne Matuszyk for testing and data contributions.

REFERENCES

1. T. Cassagne, F. Vaillant, P. Combrade, Proc. of the Eighth International Symposium on Environmental Degradation of Materials in Nuclear Power Systems-Water Reactors, p.307, August 1997.
2. R.S. Pathania, A.R. McIlree, Proc. of the Third International Symposium on Environmental Degradation of Materials in Nuclear Power Systems-Water Reactors, p.551, 1987.
3. T. Magnin, J.M. Boursier, D. Noel, F. Vallant, Proc. of the Sixth International Symposium on Environmental Degradation of Materials in Nuclear Power Systems-Water Reactors, p.669, 1993.
4. G. Economy, P.W. Pement, Corrosion 89, Paper 493, 1989.
5. T. Cassagne, A. Gelpi, Proc. of the Sixth International Symposium on Environmental Degradation of Materials in Nuclear Power Systems-Water Reactors, p.679, 1993.
6. D.S. Morton, D. Gladding, M.K. Schurman, C.D. Thompson, Proc. of the Eighth International Symposium on Environmental Degradation of Materials in Nuclear Power Systems-Water Reactors, p.387, August 1997.
7. C.D. Thompson, D.M. Carey, N.L. Perazzo, Proc. of the Eighth International Symposium on Environmental Degradation of Materials in Nuclear Power Systems-Water Reactors, p.366, August 1997.
8. M.E. Indig and C. Groot, Corrosion, Vol. 25, p.455, 1969.
9. P. Combrade, Proceedings of EPRI Alloy 600 Expert Meeting, April 6-9, 1993.
10. R.B. Rebak, Z.S. Smialowska, Corrosion, Vol. 47, p.754, 1991.
11. N. Lewis, W.J.S. Yang, J.S. Fish and D.J. Perry, C.D. Thompson, Proc. of the Eighth International Symposium on Environmental Degradation of Materials in Nuclear Power Systems-Water Reactors, p.266, August 1997.
12. S.E. Ziemniak, Journal of Solution Chemistry, Vol. 21, p. 745, 1992.
13. S.E. Ziemniak, M.E. Jones, K.E.S. Combs, Journal of Solution Chemistry, Vol. 24, p.837, 1995.

TABLE 1
MATERIAL COMPOSITION FOR ALLOYS 600, X-750 AH and X-750 HTH

Element	Alloy 600 ⁽¹⁾ Heat NX5853G11	X-750 AH Heat 38F3X	X-750 HTH Heat 84111
C	0.07	0.05	0.039
Mn	0.25	0.15	0.07
Fe	7.76	7.09	7.93
S	< 0.001	0.007	0.001
Si	0.29	0.24	0.05
Cu	0.11	0.23	0.01
Ni	75.40	72.60	72.43
Cr	15.54	15.75	15.54
Al	0.17	0.61	0.79
Ti	0.35	2.39	2.60
Mg	0.01	NR	NR
Co	0.04	0.05	0.04
P	0.007	NR	0.007
B	0.003	NR	NR
Nb+Ta	NR	NR	0.86
Sn	NR	NR	0.001
V	NR	NR	0.04
As	NR	NR	0.001
Sb	NR	NR	0.001
Bi	NR	NR	0.001

Notes to Table 1

(1) Heat NX5853G11 was tested in the mill-annealed condition.

(2) NR - not reported.

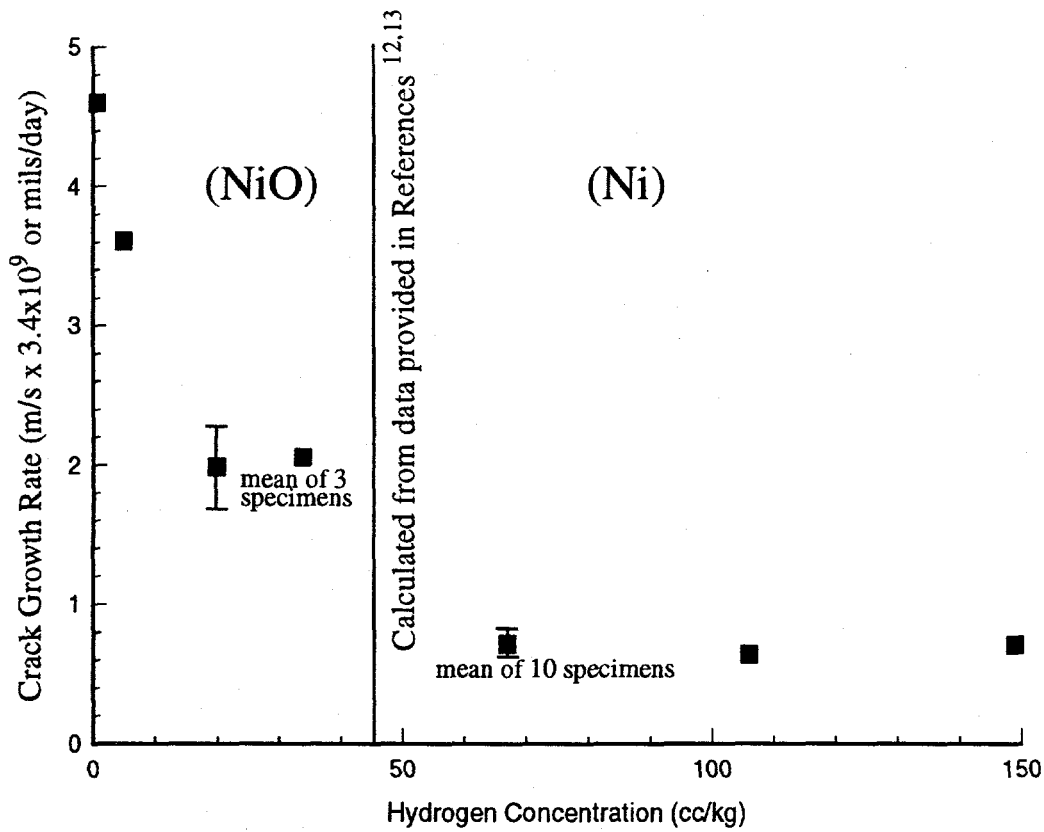


FIGURE 1: X-750 AH Heat 38F3X Average SCCGR Results 338°C, 28MPa√m

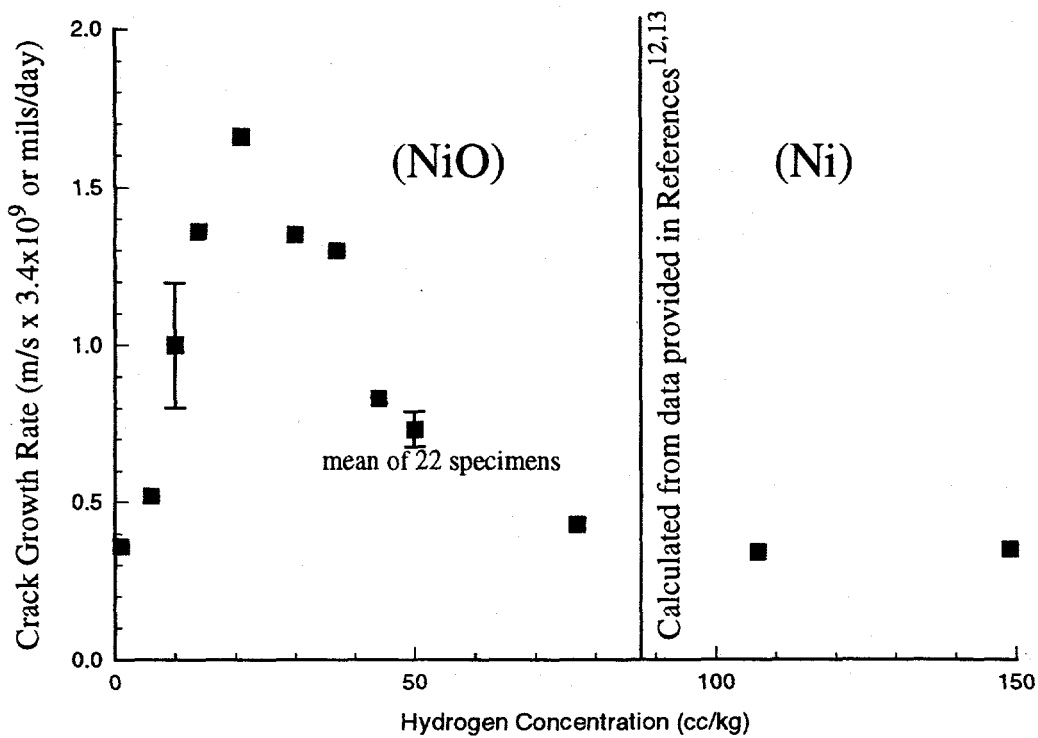


FIGURE 2: X-750 HTH Heat 84111 Average SCCGR Results 360°C, 49MPa√m

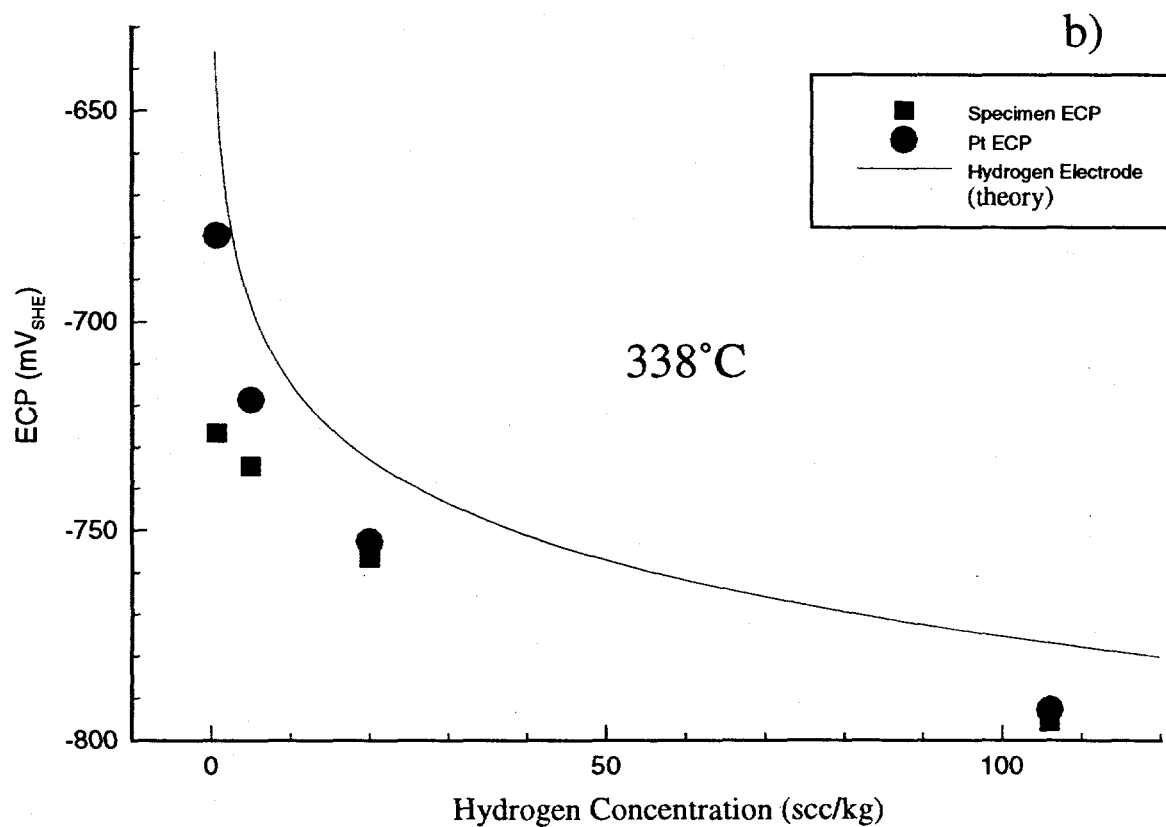
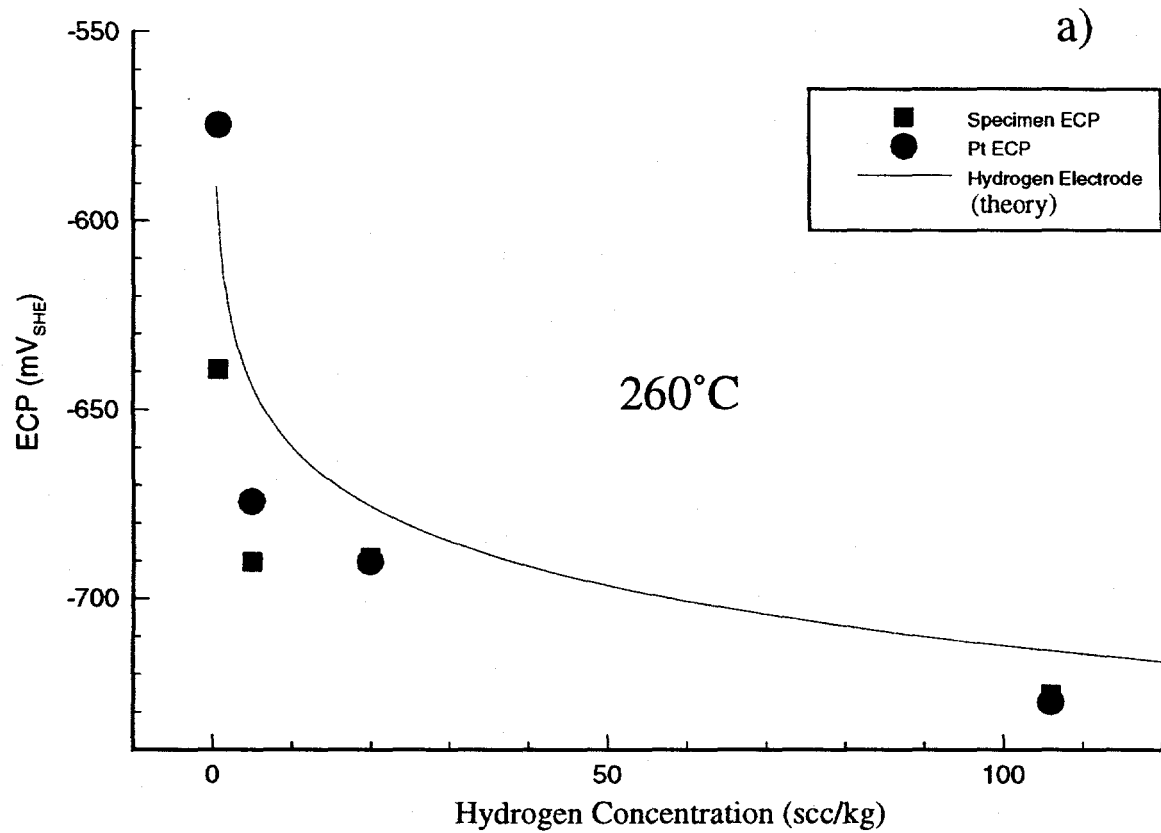


FIGURE 3: ECP vs. Hydrogen Level

c)

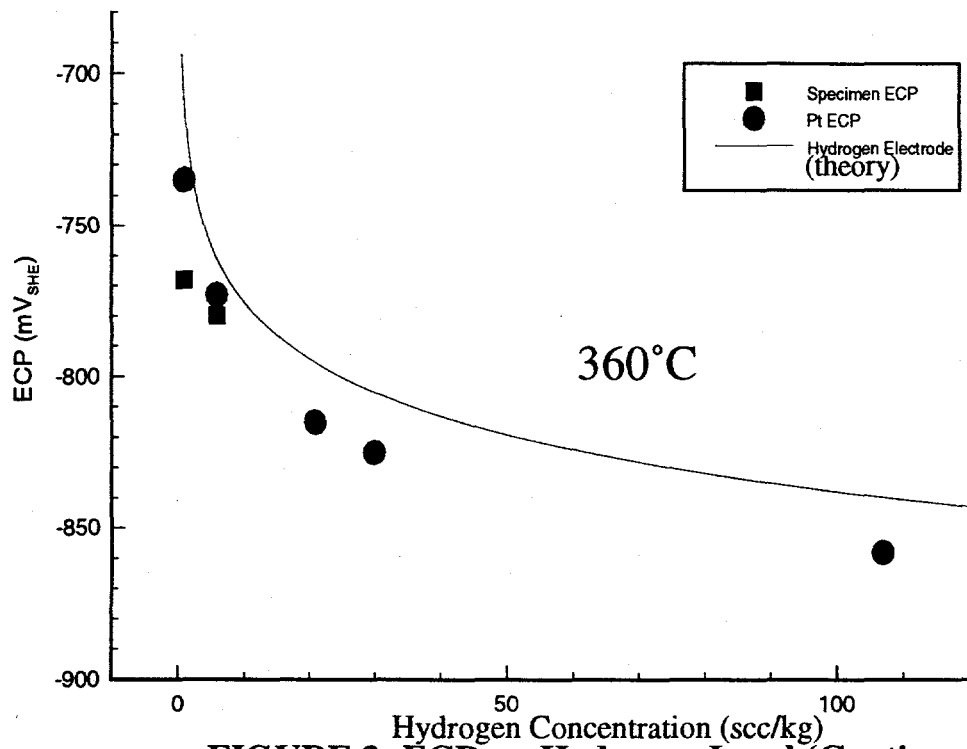


FIGURE 3: ECP vs. Hydrogen Level (Continued)

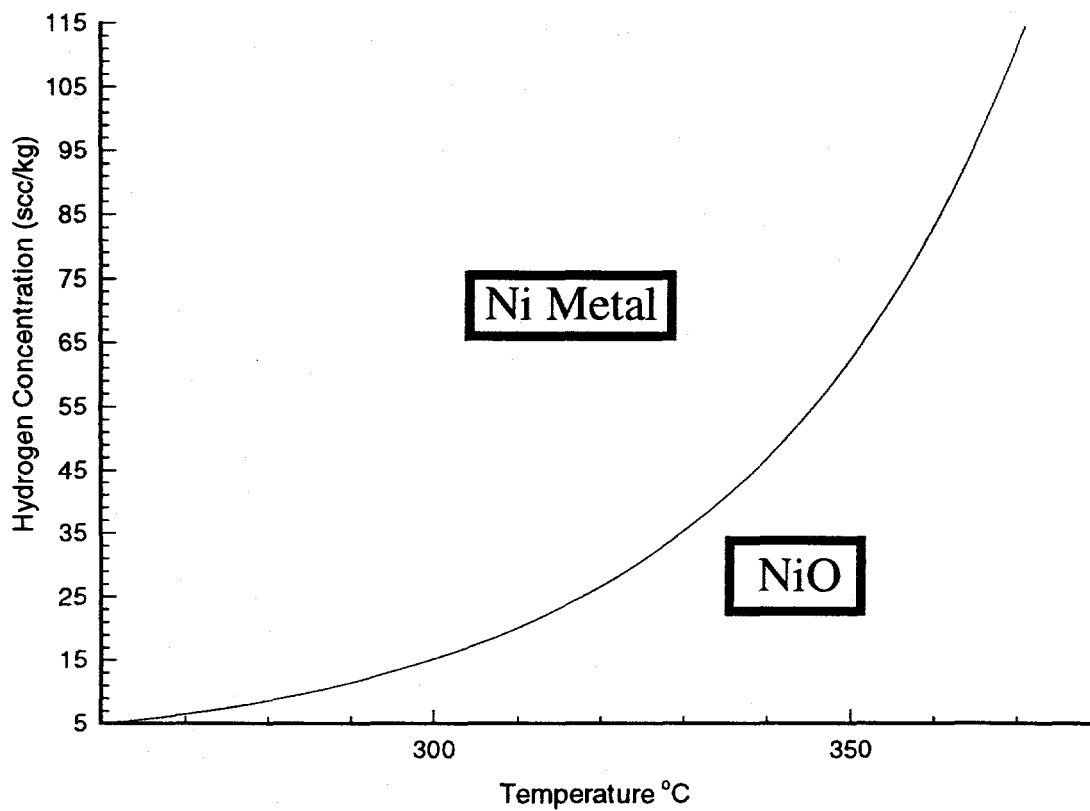


FIGURE 4: NiO/Ni Equilibrium Thermodynamic Properties from References^{12,13}

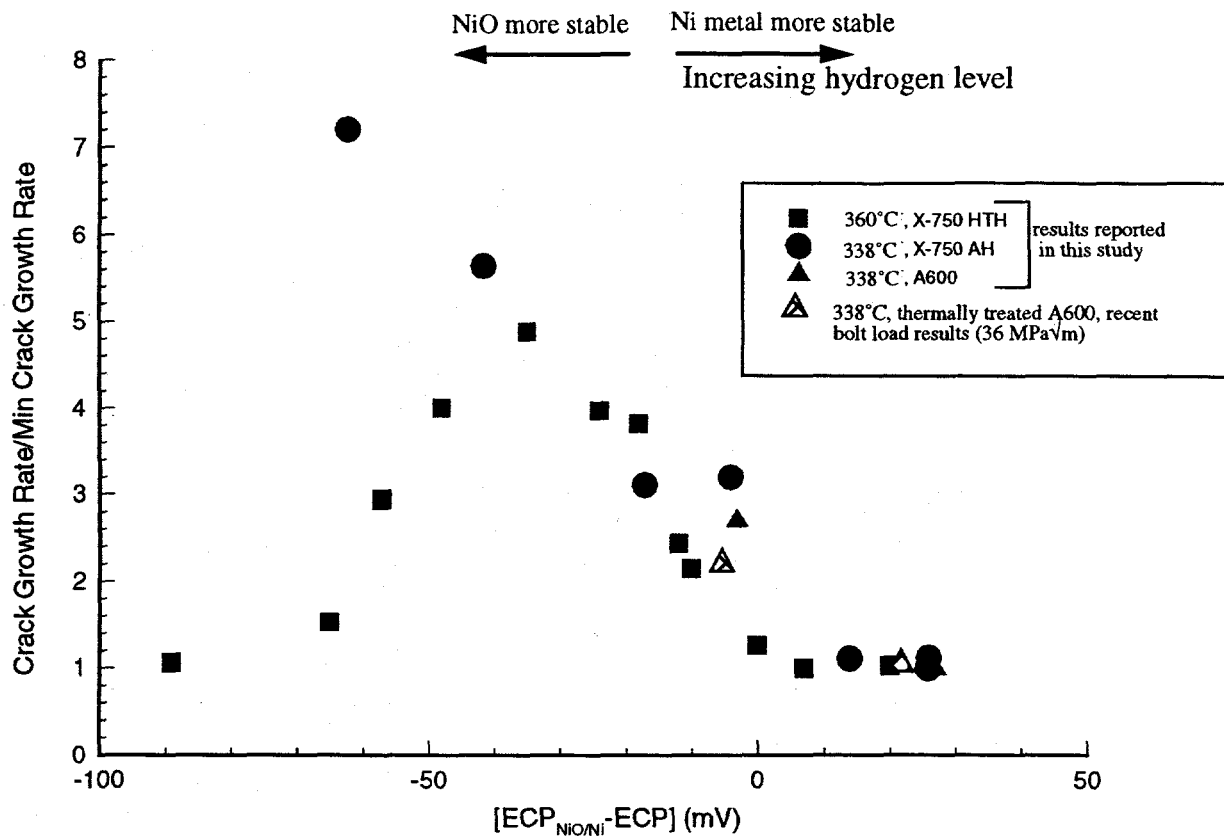


FIGURE 5: Normalized SCCGR vs. Relative Crack Tip Oxide Stability

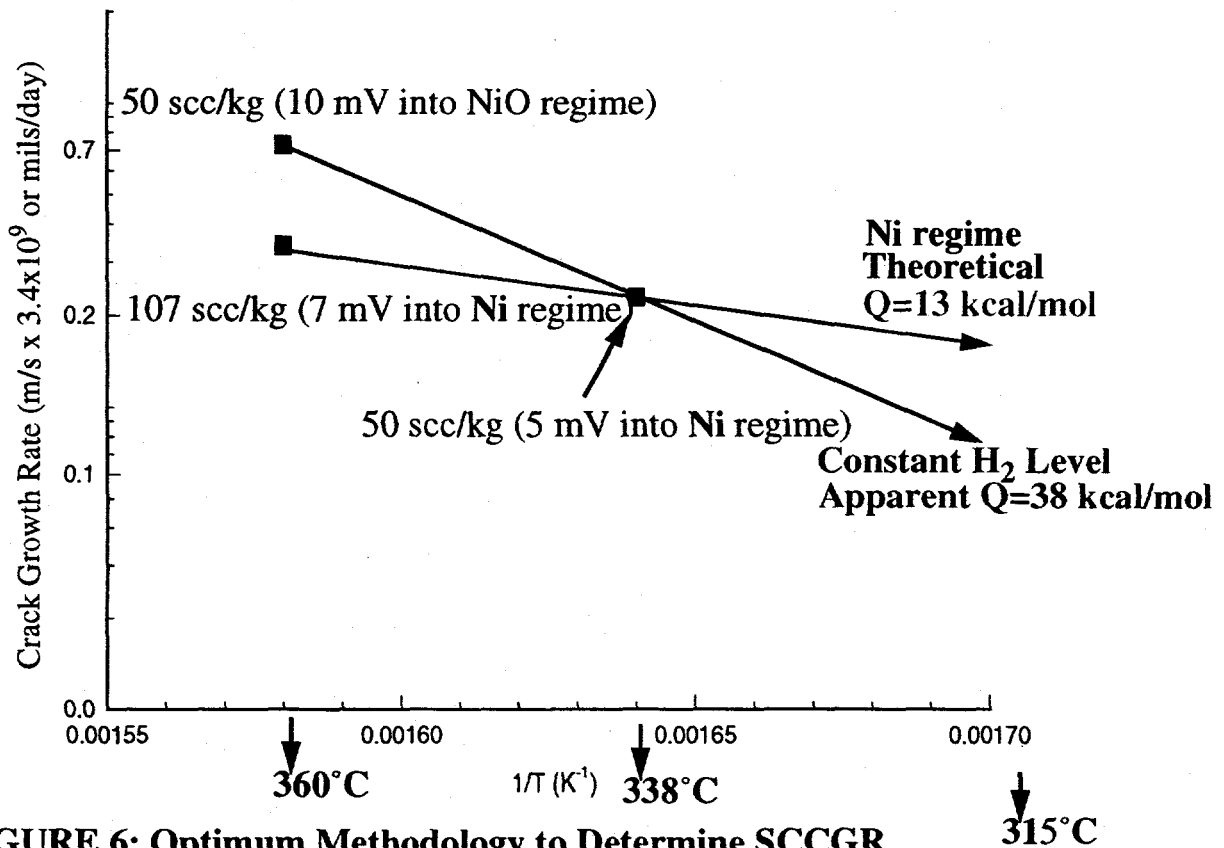


FIGURE 6: Optimum Methodology to Determine SCCGR Thermal Activation Energies (X-750 HTH Heat 84111)